

Active Magnetic Bearings with Position and Flux Observer

Angelo Bonfitto^a, Lester D. Suarez^a, Andrea Tonoli^a

^a Laboratorio di Meccatronica – Politecnico di Torino,
Corso Duca degli Abruzzi 24, 10129 Torino, Italy, andrea.tonoli@polito.it

Abstract — Standard Active Magnetic Bearings are controlled using a current reference and the measured or observed current as state variable in the state space controller. Nevertheless since this approach selects the current as the state expressing the behavior of the magnetic bearing, several disadvantages occur. Indeed it is well known that this method leads to an inherent nonlinear relation between the generated force, the current and the air gap. This paper presents the modeling approach, the control design and the experimental validation of a strategy based on the combined observation of position and flux. The technique is designed and tested on a one-degree of freedom mechanical oscillator actuated by a couple of opposite electromagnets.

I. INTRODUCTION

Contact-free levitation of rotors by means of active magnetic bearings has been a research topic for more than two decades. During this time, AMB evolved into an industry product that is used in many practical applications due to its numerous advantages over conventional bearings technology. The spread of this technology is mostly due to the growing demand of high accuracy and precision in industrial applications [1,2].

Currently the research effort is focused on many aspects of the whole suspension system i.e. power electronics, sensors, control layouts and actuators morphology, the aims being performance optimization and costs reduction.

Among these topics the definition of smart architectures allowing to optimize performance minimizing the use of sensors or getting rid of them at all is of great interest [3,4,5,6,7].

Many sensorless layouts have been developed and are currently used in industrial applications. The most spread architectures use AMB controlled with no gap sensors so to save costs and size and improve performance thanks to the inherent collocation of sensing and actuators [8,9,10,11,12].

In this paper the modeling approach, the control design and the experimental validation of a control technique based on the combined observation of position and flux is illustrated. A one-degree of freedom mechanical oscillator actuated by a couple of electromagnets has been used to test the effectiveness of the proposed control strategy. The proposed

layout exploits an observer to estimate the mechanical position, velocity and the flux on the electromagnets starting from current and position direct measurements. A cascaded control layout uses the flux observation in an inner flux loop whose reference is provided by the external position loop closed on the observed position.

As well known, the first advantage of a flux feedback approach is to minimize the effect of the displacement on the actuation force. Additionally, this layout allows to minimize the amount of noise introduced in the control loops. The model based observer approach permits to estimate the dynamics of interest, reducing noise issues and the effects of high order dynamics that are considered useless in terms of control performance.

Furthermore, the possibility of using the electromagnet either as actuator and sensor, permits to overcome actuators/sensors non-collocation problems, typical in rotors control layouts using direct position sensing as feedback in closed loops.

The overall system results to be more efficient than standard control layouts since it avoids measurements noise in the control loops while generating a system characterized by actuator/sensor collocation and using a linear formulation of the force generated by the electromagnets.

The paper starts on the description of modeling phases, details the steps followed for observer design and treats the selection of filters dynamics for both inner and outer control loops.

Afterwards the comparison of numerical and experimental results is presented aiming to validate the modeling approach of the mechanical and electrical subsystems and their interactions and to prove the effectiveness of the control action along with the performance and the efficiency of the resulting system.

The paper concludes providing an outlook on the next steps in the refinement of this scheme that will be mostly focused on the improvement of control architecture and of the model so to take into account hidden information such as magnetization or hysteresis of the core iron material, stray flux and eddy currents. The natural application of the presented technique is its transfer to the control of rotors suspended by means of active magnetic bearings.

II. MODELING AND CONTROL DESIGN

The considered system is a one degree of freedom mass-spring oscillator actuated by two opposite electromagnets, corresponding to an AMB configuration, as shown in Figure 1. The electromagnets are assumed to be identical, and the coupling between the two electromagnetic circuits is neglected. Also, each electromagnet can be considered as a two-port element (electrical and mechanical).

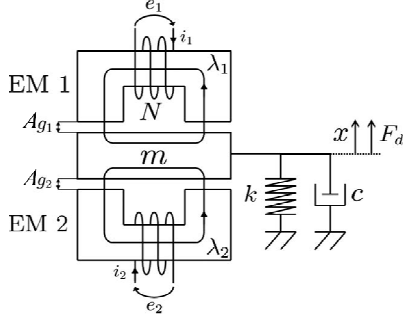


Figure 1. Model.

Owing to Newton's law in the mechanical domain and the Faraday and Kirchoff laws in the electrical domain, the dynamics equations of the system are

$$\begin{aligned} m\ddot{x} + c\dot{x} + kx &= F_j \\ \dot{\lambda}_j + Ri_j &= e_j \pm k_m \dot{x} \quad , j=1,2 \end{aligned} \quad (1)$$

where R is the coils resistance, c the viscous damping, k the stiffness, λ_j is the total flux and e_j , i_j and F_j are the voltage, current and force for each electromagnet j . The force F_j can be derived from the energy store E_j in the electromagnet.

$$\begin{aligned} E_j(i_j, x_j) &= \frac{1}{2} \frac{\lambda_j^2}{L(x)} \\ F_j(i_j, x_j) &= \frac{\partial E_j(i_j, x_j)}{\partial x} \quad , j=1,2 \end{aligned} \quad (2)$$

Thus, the generated force related to the control flux can be expressed as

$$F_j = \frac{\lambda_j^2}{\mu_0 Ag} \quad , j=1,2 \quad (3)$$

where Ag is the nominal airgap and μ_0 is the permeability.

The system dynamics is linearized around a working point corresponding to a bias flux λ_0 imposed to both electromagnets (Eq. 4)

$$\lambda_j = \lambda_0 \pm \lambda_c \quad , j=1,2 \quad (4)$$

$$\begin{aligned} m\ddot{x} + c\dot{x} + kx &= \frac{1}{\mu_0 Ag} [\lambda_1^2 - \lambda_2^2] \\ m\ddot{x} + c\dot{x} + kx &= \frac{1}{\mu_0 Ag} [(\lambda_0 + \lambda_c)^2 - (\lambda_0 - \lambda_c)^2] \\ m\ddot{x} + c\dot{x} + kx &= \frac{4\lambda_0}{\mu_0 Ag} \lambda_c \end{aligned} \quad (5)$$

where λ_c is the control flux.

Finally, considering a dynamic equilibrium, the mathematical model is expressed as follow

$$\begin{aligned} m\ddot{x} + c\dot{x} + kx &= \frac{4\lambda_0}{\mu_0 Ag} \lambda_c \\ \dot{\lambda}_j + \frac{R}{L} \lambda_j &= e_j \pm k_m \dot{x} \quad , j=1,2 \end{aligned} \quad (6)$$

A three-state-space model is used to study system dynamics described in Eq. 7. The resulting linearized state-space model can be represented as follows:

$$\begin{aligned} \dot{\mathbf{X}} &= \mathbf{A}\mathbf{X} + \mathbf{B}u \\ \mathbf{y} &= \mathbf{C}\mathbf{X} \end{aligned} \quad (7)$$

where \mathbf{A} , \mathbf{B} , and \mathbf{C} are the dynamic, action, and output matrices, respectively, defined as

$$\begin{aligned} \mathbf{A} &= \begin{bmatrix} 0 & 1 & 0 \\ -k/m & -c/m & 4\lambda_0/(m\mu_0 Ag) \\ 0 & -k_m & -R/L \end{bmatrix} \\ \mathbf{B} &= \begin{bmatrix} 0 \\ 0 \\ 1 \end{bmatrix}, \quad \mathbf{C} = \begin{bmatrix} 1 & 0 & 0 \\ 0 & 0 & 1/L \end{bmatrix} \end{aligned} \quad (8)$$

with the associated input and output state vectors $\mathbf{X} = \{x, \dot{x}, \lambda\}^T$, $u = e_0$ and $\mathbf{y} = \{x, \lambda\}^T$

TABLE I. MODEL PARAMETERS

Parameter	Value	Unit
R	Coils resistant	0.356 Ω
L	Coils inductance	5.8e-3 H
Ag	Airgap	0.6e-3 mm
μ_0	permeability	1.25e-6 H/m
m	mass	3.41 Kg
k_m	Back-FEM	3.96 Vs/rad
c	Viscous damping	1.15 kg/s
k	Stiffness	46500 kg/s ²

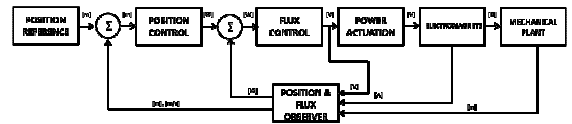


Figure 2. System Control Layout

The overall control scheme is illustrated in Figure 2. Here, the position and flux observer estimates the state variables based on the measurement of the output and control variables to generate the desired control vector.

From the system defined by Eq. 7, the dynamic model of the state observer can be obtained assuming that the state vector \mathbf{X} is approximated by the observed state vector $\hat{\mathbf{X}}$

$$\dot{\hat{\mathbf{X}}} = \mathbf{A}\hat{\mathbf{X}} + \mathbf{B}\mathbf{u} + \mathbf{L}(\mathbf{y} - \mathbf{C}\hat{\mathbf{X}}) \quad (9)$$

$\mathbf{L}(\mathbf{y} - \mathbf{C}\hat{\mathbf{X}})$ is a correction term that involves the difference between the measured output \mathbf{y} and the estimated output $\mathbf{C}\hat{\mathbf{X}}$ to minimize the difference between the dynamic model and the actual system. Thus, the problem of designing a state observer becomes that of determining the observer gain matrix \mathbf{L} such that the error dynamic is asymptotically stable with sufficient speed of response. Furthermore, the asymptotically stability and the speed of response is determined by the eigenvalues of matrix $(\mathbf{A} - \mathbf{L}\mathbf{C})$

III. EXPERIMENTAL SETUP

The system used for the experimental investigation is a test rig available at the Mechatronics Laboratory of Politecnico di Torino presented in Figures 3 and 4. It is used for static characterization of radial magnetic bearings and for the analysis of different control strategies, sensors, and power amplifiers in a simple and well known experimental setup without the need of an expensive prototype of the whole suspension. This rig consists in a horizontal arm hinged at one extremity with a pivot and actuated with a single axis magnetic bearing. The electromagnets have 142 windings, an airgap area $S=4.2 \times 10^{-4} \text{ m}^2$, and a nominal airgap of approximately $g=0.6 \text{ mm}$.

The length of the pendulum (320 mm) compared with the

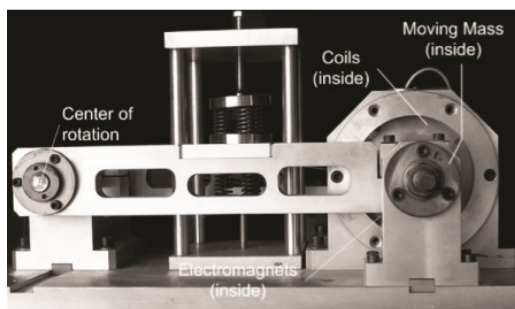


Figure 3. Picture of test rig

nominal airgap insures that the circular motion of the mass can be approximated with a linear translation (x). The base plate, connecting arms, and electromagnets' housing are made of aluminum, while the shafts are made of steel. The ferromagnetic circuit (stator and moving part) of the electromagnet is made of silicon iron sheets. Six springs in parallel are located at a distance of 160 mm from the hinge to provide a stabilizing stiffness to the system if necessary.

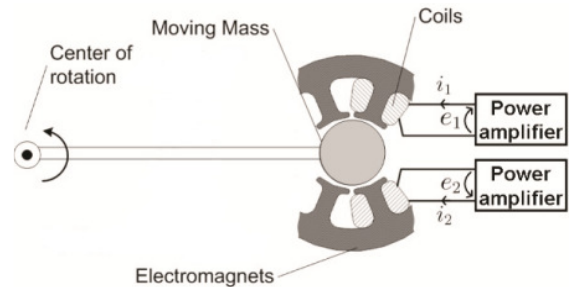


Figure 4. Picture of test rig

A DSP TI TMS320F28335 has been used for the control implementation. The analog-to-digital converters use 12 bit over a range of 3 V, with a sampling rate of 40 kHz.

The position was measured with a Bently Proximito 3300XL eddy current sensor just for monitoring and validation, and not for feedback purposes. AMP25 Hall current sensors (range $\pm 5\text{A}$) were used for the current measurement in the two coils (lower than 100 mA, peak-to-peak, of noise).

The V_{dc} value of the power amplifier was set to 20 V, and the switching frequency was set to 40 kHz. Thus, as both the sampling rate and the switching frequency of the PWM were far beyond the mechanical frequency of the system (around 20 Hz), their dynamics was neglected during the study.

IV. EXPERIMENTAL RESULTS

The proposed technique has been validated experimentally so to verify that the proposed technique allows to avoid the direct effect of displacement on the actuation force typical of architecture with current feedback. To this end, after a preliminary phase of electromechanical parameters identification, an impact test with the external position loop disabled and the internal one (in current or in flux) enabled has been performed. To execute these tests, the plant has been mechanical centered by means of a set of springs (k in Table I). Results show that with electromagnets off, the system oscillates at a frequency of round 20 Hz (Figure 5.a). When the current loop is enabled with a bias of 0.5 A, the system oscillates at 15 Hz (Figure 5.b), while with the flux feedback the effects of negative stiffness disappears and the oscillation returns to be 20 Hz (Figure 5.c). The comparison between the three tests is reported in Figure 6.

The second phase of experimental tests is focused on the verification of system behaviour in closed loop configuration. The mechanical spring are uninstalled and the impact tests leads to results illustrated in Figure 7.

A further advantage of the proposed technique is the possibility of using observed position as feedback in the external loop. As a matter of fact this procedure acts as a filter against high frequency noise. Figure 9 shows the difference between the closed loop response obtained feed-backing measured position (a) and observed position (b). Apart from noise reduction, the use of a model based estimator could give benefits in terms of robustness in the presence of failure of one of the sensors.

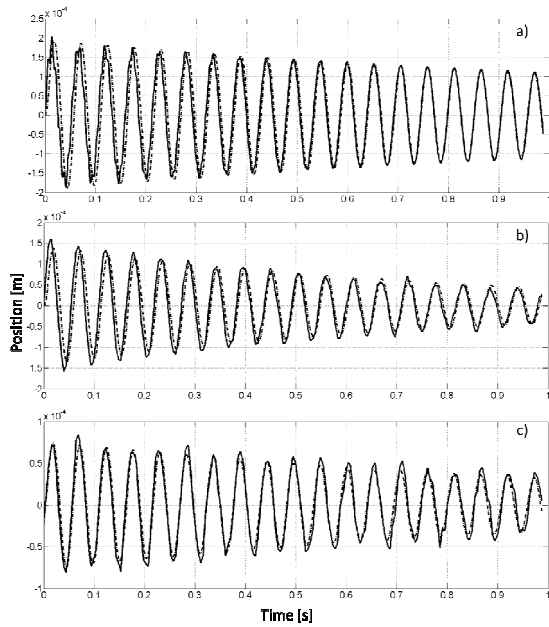


Figure 5. Tests with external position loop disabled and internal loop enabled. (Bias 0.5 A). Experimental (solid line) vs numerical results (dash-dotted lines). a) electromagnets off; b) internal current loop; c) internal flux loop.

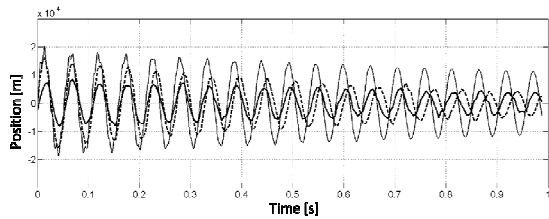


Figure 6. Tests with external loop disabled. Electromagnets off (solid thin line) vs Current feedback (dashed line) vs Flux feedback (solid bold line).

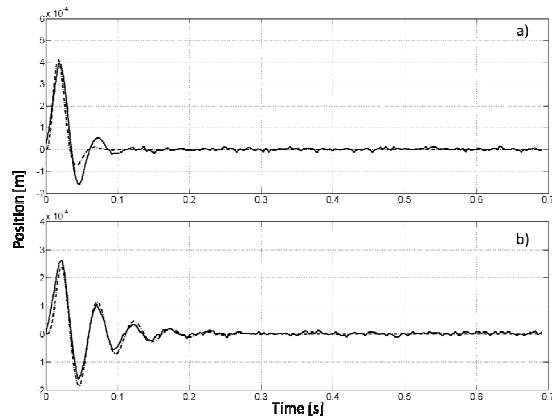


Figure 7. Test with external position loop enabled. Experimental (solid line) vs numerical results (dash-dotted lines). a) Current feedback; b) Flux feedback.

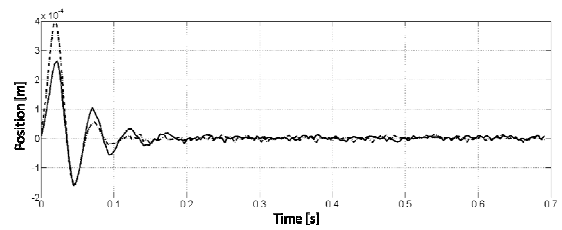


Figure 8. Test with external position loop enabled. Current feedback (dashed line) vs Flux feedback (solid line).

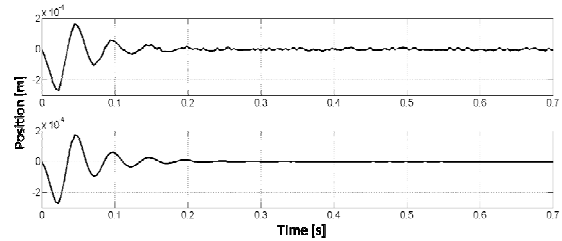


Figure 9. Closed position loop response. a) Feedback with measured position; b) Feedback with observed position.

V. CONCLUSIONS

In this paper a technique of AMB control based on observed flux feedback has been presented. Starting from the measurement of mechanical displacement, current and voltage, the observer allows to estimate the flux and the position itself so to perform a cascaded control allowing to avoid the effect of negative stiffness on actuation force and to reduce noise by feed-backing observed position and flux. Next steps will be focused on optimization of the control layout studying a feedback action based on pole placement technique and getting rid of cascaded architecture. A further step will be the improvement of the model so to take into account hidden information such as magnetization or hysteresis of the core iron material, stray flux and eddy currents.

NOMENCLATURE

c	=	viscous damping coefficient
k	=	Stiffness
e	=	voltage applied to an electromagnet
Ag	=	Airgap
i	=	Current
k_m	=	back-electromotive force factor
m	=	mass
x	=	displacement of the mass
F	=	magnetic force
R	=	Resistance
L	=	Inductance
S	=	cross-sectional area of the magnetic circuit
λ	=	magnetic flux
μ_0	=	magnetic permeability of the vacuum
E	=	magnetic energy

REFERENCES

- [1] Bleuler H., Cole M., Keogh P., Larssonneur R., Maslen E., Nordmann R., Okada Y., Schweitzer G., Traxler A., "Magnetic Bearings Theory, Design, and Application to Rotating Machinery", Springer, Berlin Heidelberg, 2009
 - [2] Chiba A., Fukao T., Ichikawa O., Oshima M., Takemoto M., Dorrell D.G., "Magnetic Bearings and Bearingless Drives" Elsevier, Oxford, 2005.
 - [3] Tonoli, A., Bonfitto, A., De L'epine, X., Silvagni, M., 2009, "Self-sensing Active Magnetic Dampers for vibration control", *Journal of Dynamic Systems, Measurement and Control*, 131, pp.
 - [4] Vischer, D., and Bleuler, H., 1990, "A new approach to sensorless and voltage controlled AMBs based on network theory concepts," *Second International Symposium on Magnetic bearings*, 12-14 July, Tokyo, Japan, pp. 301-306.
 - [5] Noh, M. D., and Maslen, E. H., 1997, "Self-sensing magnetic bearings using parameter estimation," *IEEE Trans. Instr. Meas.*, 46(1), pp. 45-50.
 - [6] Schammass, A., Herzog, R., Buhler, P., and Bleuler, H., 2005, "New results for self-sensing active magnetic bearings using modulation approach," *IEEE Trans. Contr. Syst. Tech.*, 13(4), pp. 509-516.
 - [7] Mizuno, T., Araki, and K., Bleuler, H., 1996, "Stability analysis of self-sensing magnetic bearing controllers," *IEEE Trans. Contr. Syst. Tech.*, 4(5), pp. 572-579.
 - [8] H. Bleuler, D. Vischer, Schweitzer T., Traxler A., Zlatnik D. "New Concepts for cost-effective Magnetic Bearings Control" *Automatica*, vol. 30 no. 5, pp.871-876, 1994.
 - [9] Mizuno, T., Namiki, H., and Araki, K., 1996, "Self-sensing operations of frequency-feedback magnetic bearings," *Fifth International Symposium on Magnetic Bearings*, 29-30 Aug., Kanazawa, Japan, pp. 119-123.
 - [10] Okada, Y., Matsuda, K., and Nagai, B., 1992, "Sensorless magnetic levitation control by measuring the PWM carrier frequency component," *Third International Symposium on Magnetic Bearings*, 21-31 July, Radisson Hotel, Alexandria, VA.
 - [11] Mizuno, T., Ishii, T., and Araki, K., 1998, "Self-sensing magnetic suspension using hysteresis amplifier," *Cont. Eng. Pract.*, 6, pp. 1133-1140.
- Vischer, D., and Bleuler, H., 1993, "Self-sensing magnetic levitation," *IEEE Trans. on Magn.*, 29(2), pp. 1276-1281.